Available online at www.ijournalse.org

Emerging Science Journal

(ISSN: 2610-9182)

Vol. 9, No. 2, April, 2025

Effect of Antenna Polarization Arrangement on MIMO Channel Capacity

Trasma Yunita [1*], Harfan H. Ryanu [1], Aloysius A. Pramudita [1]

[1] *The University Center of Excellence for Intelligent Sensing-IoT, Telkom University, Bandung 40257, Indonesia.*

Abstract

This study investigates the effect of antenna polarization configurations on the channel capacity of Multiple-Input Multiple-Output (MIMO) systems. Theoretical modeling and computational simulations are conducted to examine the impact. The theoretical model is predicated on a MIMO arrangement with a half-wavelength Dipole antenna as the MIMO element. The influence of antenna polarization on MIMO capacity is expressed via mutual impedance as a function of antenna polarization. Theoretical and simulation results indicate that antenna polarization influences the capacity of MIMO channels. Cross-polarized antenna arrays provide enhanced polarization by optimizing polarization diversity. Research on large-scale MIMO systems suggests that the selection of antenna polarization significantly influences MIMO channel capacity. The polarization configuration substantially influences MIMO capacity under high SNR scenarios. An appropriate polarization configuration enhances MIMO channel capacity at low signal-to-noise ratio (SNR) more efficiently than inappropriate polarization. This may be advantageous in mitigating capacity degradation resulting from low SNR levels. Furthermore, the research findings indicate that the antenna polarization configuration is essential in designing massive MIMO antennas comprising several antennas. In creating a massive MIMO antenna, achieving the ideal polarization configuration of the antenna elements is critical to ensure that increases in the number of antennas correlate with the optimum channel capacity.

Keywords:

Massive MIMO;
Antenna Polarization;
Channel Capacity;
Mutual Impedance;
Optimum Arrangement.

Article History:

Received:	14	October	2024
Revised:	09	March	2025
Accepted:	16	March	2025
Published:	01	April	2025

1- Introduction

The growing number of wireless communication applications and technologies has increased the demand for wireless throughput. These include the Internet of Things, wireless sensor networks, and augmented reality. A method used to meet the capacity demands of wireless communication is to expand bandwidth; however, this is a traditional approach that necessitates considerable work. An alternative approach involves employing a multiple-input multiple-output (MIMO) system, which utilizes several antennas at both the transmission and reception terminals. MIMO systems enhance the spectral efficiency of wireless communications under defined bandwidth and total power constraints [1, 2]. MIMO systems have been included in wireless communication technologies, including wireless LAN, third-generation (3G), and fourth-generation (4G) mobile networks. As the demands for wireless bandwidth increase, numerous research initiatives dedicated to enhancing 5G wireless communication technology have focused on addressing this capacity constraint. A current research emphasis on this capacity constraint is massive MIMO, which investigates the feasibility of employing many antennas at a wireless base station [2-4].

In MIMO systems, two prerequisites must be satisfied to leverage the system's advantages. The first criterion is a significant scattering environment, followed by the necessity of accurate channel state information (CSI) at the receiver end [5, 6]. MIMO antenna systems have garnered considerable interest in contemporary wireless communications

* **CONTACT**: trasmayunita@telkomuniversity.ac.id

DOI: http://dx.doi.org/10.28991/ESJ-2025-09-02-028

because they can enhance spectral efficiency, elevate data rates, and mitigate the impacts of fading and interference [7, 8]. The extensive scattering environment enhances the capacity of MIMO systems since the MIMO channel can be divided into a more significant number of parallel independent channels when the correlation between various transmitter and receiver antenna pairs is diminished [9-12]. The effect of antenna characteristics on MIMO system capacity was examined utilizing the previously discussed monopole array configuration by Hui [13]. From the perspective of antenna design, the spatial correlation among channels in a MIMO system can be associated with the mutual coupling between antenna elements. Previous research studies suggest that mutual coupling influences MIMO capacity [14-18]. The design process of MIMO systems requires consideration for mutual interaction between antenna elements on both the transmitting and receiving ends. This is particularly crucial for massive MIMO to ensure a significant enhancement in system capacity.

The mutual coupling between elements in an antenna array is mainly determined by the inter-element distance, the radiation pattern, and the polarization of each component [19, 20]. A substantial separation between elements in an antenna array will yield minimal mutual coupling; nevertheless, the overall dimensions of the array will be considerably more significant. Mutual coupling can be defined as the impedance between the transmitting and receiving antennas. Prior research concerning MIMO antenna design argues for low mutual coupling characteristics as a criterion in the antenna design process [19-23]. Numerous decoupling techniques exist to enhance antenna isolation and achieve minimal mutual coupling, which is crucial for developing MIMO antennas. Numerous studies have established decoupling techniques utilized for MIMO antennas. Previous papers present examples of recently investigated decoupling methods, including Defected Ground Structure (DGS) [24, 25], metamaterial structures [26, 27], pattern diversity approaches [28], and transmission line techniques [29]. Other physical characteristics of wave propagation, including polarization, are also considered in the design of MIMO systems to achieve minimal mutual coupling values [30-32]. Antenna polarization is utilized to achieve less mutual coupling and enhance the diversity of MIMO systems. The influence of antenna polarization and propagation path on wave polarization in a MIMO channel necessitates more investigation into the correlation between mutual coupling and MIMO capacity and the impact of antenna polarization on the mutual impedance between antennas. Consequently, polarization configurations among elements in a MIMO antenna must be considered when designing linear polarization antennas, such as Dipole antennas, to ensure that the antenna polarization orientation aligns with the antenna orientation. The relative angles of two adjacent Dipole antenna orientations are variables that influence the mutual impedance between the elements [19]. This research examines the polarization configuration between antennas in a MIMO system and its impact on MIMO capacity. The primary contributions of this study are as follows:

- The optimum antenna polarization configuration will enhance the MIMO capacity when utilizing a MIMO antenna with a specific number of antenna elements. The ideal configuration of antenna polarization is used as an indicator for establishing the MIMO antenna design. A mathematical model addressing the antenna polarization effect on MIMO capacity is suggested and analyzed, with computer simulations performed to validate the findings.
- The arrangement of antenna polarization has a more substantial impact on MIMO capacity with numerous antennas than a limited number of antennas in a MIMO system. The optimal configuration may mitigate the capacity decrease resulting from poor SNR. Consequently, it is essential to include this in designing a large MIMO antenna to get adequate capacity.

This paper is organized as follows: Section 1 introduces the motivation for studying the effect of antenna polarization on MIMO capacity. Section 2 describes the theoretical analysis, which contains the derivation of MIMO capacity calculations related to the impact of polarization arrangement. Section 3 discusses the resulting analysis, which covers several potential arrangements at different SNR conditions. Section 4 provides the conclusion of the entire study in the preceding sections.

2- Polarization Arrangement and Channel Capacity Overview

Section 2 of the paper defines this study's numerical methodology and formulas. The effect of polarization arrangement in MIMO antennas on system channel capacity is investigated according to the flowchart in Figure 1. Beginning with the characterization of MIMO antenna elements, including their dimensions, inter-element spacing, and angular orientation, proceeding to the computation of system capacity based on the associated SNR value. In practical systems, enhancing SNR increases spectral efficiency only to a certain threshold. Hardware limitations, interference, and deficiencies in modulation and coding result in actual efficiency regularly falling short of the theoretical maximum. In this work, the SNR values employed range from 5 to 25 dB, covering both low (5-15 dB) and good (16-25 dB) conditions as defined by ITU-R and FCC technical standards. Then, the mutual impedance value will change in each antenna configuration due to variations in the mutual coupling value resulting from the polarization arrangement. The spatial correlation value must be calculated initially for measurement. Subsequently, the channel matrix and channel capacity are determined. Then, the results are expected to apply to specific applications, including 5G base stations and satellite communication systems [33].

Figure 1 shows the flowchart of the research methodology through which the objectives of this study were achieved.

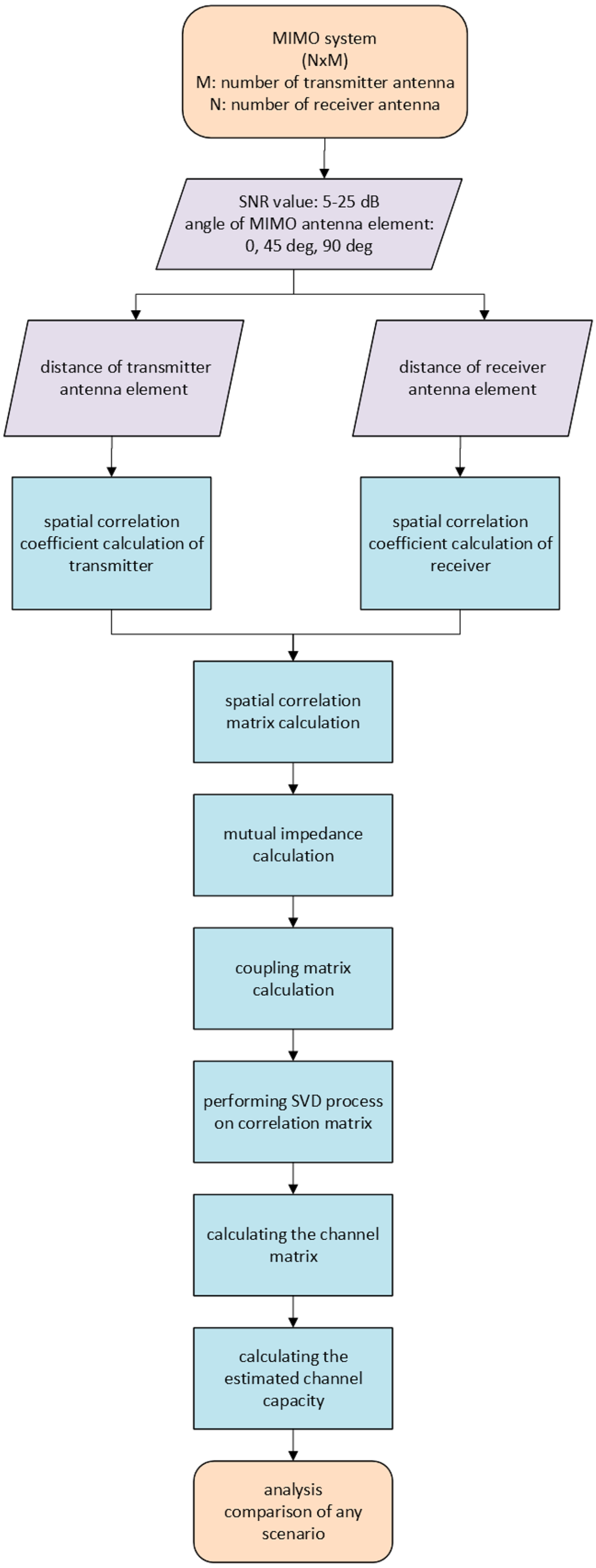

Figure 1. Methodology Flowchart

A MIMO system is characterized by M antennas on the transmitter and N antennas on the receiver. The channel gain coefficients are denoted as h_{ba} and h_{dc}, representing the gain between the a^{th} and c^{th} antenna on the transmitter and the b^{th} and d^{th} antenna on the receiver, where a and c range from 1 to M, then b and d range from 1 to N. As explained by Hui [13], the spatial correlation coefficient between the channels of two pairs of transmitting and receiving antennas can be expressed as Equation 1.

$$\rho_{ba,dc} = \frac{E(h_{ba}h_{dc}^*)}{\sqrt{E(h_{ba}h_{ba}^*)E(h_{dc}h_{dc}^*)}} \tag{1}$$

The channel coefficient is the ratio between the open-circuit voltage at the receiver antenna terminal and the excitation voltage at the transmitter antenna. Furthermore, h_{ba} and h_{dc} are determined as Equation 2.

$$h_{ba} = \frac{V_{ob}}{V_a}, h_{dc} = \frac{V_{od}}{V_c} \tag{2}$$

With V_{ob} and V_{od} are open-circuit voltages at b^{th} and d^{th} receiver antenna. V_a and V_c are the excitation voltage at a^{th} and c^{th} transmitter antenna. Concerning Equation 2 and assuming the values of V_{ob} and V_{od} are deterministic, then the cross-correlation between them can be written as Equation 3:

$$E(V_{ob}V_{od}^*) = E\left\{\begin{aligned}&\left[-\frac{1}{I_{ob}}\int_0^{2\pi}\int_0^{L} J_a(l).\left(\int_0^{2\pi} E_{ta}(\phi)\,d\phi\right).E_{rb}(\phi)dld\phi\right].\\&\left[-\frac{1}{I_{ob}}\int_0^{2\pi}\int_0^{L} J_c(l).\left(\int_0^{2\pi} E_{tc}(\phi)\,d\phi\right).E_{rd}(\phi)dld\phi\right]\end{aligned}\right\} \tag{3}$$

where J_a is the current distribution of the a^{th} element of the transmitting antenna, $E_{ta}(\phi)$ is the electric field that is transmitted by the antenna, $E_{rb}(\phi)$ is the incident electric field on the b^{th} element of the receiving antenna, J_c is the current distribution of the c^{th} element of the transmitting antenna, $E_{tc}(\phi)$ is the electric field that is transmitted by the antenna, and $E_{rd}(\phi)$ is the incident electric field on the d^{th} element of the receiving antenna, respectively. Due to the random process of the channels, $E_{rb}(\phi)$ and $E_{rd}(\phi)$ can be assumed as a random complex Gaussian. L is Dipole length and I_{ob} in total current in the antenna terminal, all elements are assumed to be the same. The different positions between the transmitter and receiver antenna elements represent the phase difference between elements that depend on their distance. The electric field relation between two transmitting antennas (a and c) with a distance of d_{ac} and between two receiving antennas (b and d) with a distance of d_{bd} are written as Equation 4. Then, the cross-correlation in Equation 3 can be written as Equation 5. By considering Equation 4;

$$E_{tc} = E_{ta}e^{j\beta d_{ac}\cos(\phi')}, E_{rd} = E_{rb}e^{j\beta d_{bd}\cos(\phi')} \tag{4}$$

$$\begin{aligned}E(V_{ob}V_{od}^*) = \frac{1}{|I_{ob}|^2}&\left(\int_0^L\int_0^L J_a(l)J_c^*(l')dldl'\right)E\{|E_{ta}|^2\}E\{|E_{rb}|^2\}\\&\left(\int_0^{2\pi} e^{j\beta d_t\cos\phi'}\,d\phi'\right).\left(\int_0^{2\pi} e^{j\beta d_r\cos\phi'}\,d\phi'\right)\end{aligned} \tag{5}$$

Part of Equation 5 can be represented as a constant K, as stated in Equation 6. The double integral of the phase difference of two antennas in transmitter and receiver stated in Equation 5 can be written as zero-order Bessel functions as given in Equations 7 and 8 [18].

$$\frac{1}{|I_{ob}|^2}\left(\int_0^L\int_0^L J_a(l)J_c^*(l')dldl'\right)E\{|E_{ta}|^2\}E\{|E_{rb}|^2\} = K \tag{6}$$

$$\left(\int_0^{2\pi} e^{j\beta d_t\cos\phi'}d\phi'\right) = J_0(\beta d_t) \tag{7}$$

$$\left(\int_0^{2\pi} e^{j\beta d_r\cos\phi'}d\phi'\right) = J_0(\beta d_r) \tag{8}$$

Substituting Equations 6, 7, and 8 into Equation 5 then the cross-correlation result can be expressed as $[\![E[V]\!]_{ob}V_{od}^*] = KJ_0(\beta d_t)J_0(\beta d_r)$ and by considering the autocorrelation, each channel is a constant K ($[\![E[h]\!]_{ba}V_{ba}^*] = [\![E[h]\!]_{dc}h_{dc}^*]$. Finally, the spatial correlation coefficient between the channels of two pairs of transmitting and receiving antennas can be written as Equation 9.

$$\rho_{ba,dc} = J_0(\beta d_t) J_0(\beta d_r) \tag{9}$$

where J_0 is the first order of the Bessel function. Furthermore, the spatial correlation matrix for the $N \times M$ *MIMO* antenna that refers to the receiving and transmitting antenna can be written as Equations 10 and 11:

$$\rho_{rx\,m,b} = \begin{bmatrix} J_0(\beta d_{r\,1,1}) & J_0(\beta d_{r\,1,1}) & \cdots & J_0(\beta d_{r\,1,N}) \\ J_0(\beta d_{r\,2,1}) & J_0(\beta d_{r\,2,1}) & \cdots & J_0(\beta d_{r\,2,N}) \\ \vdots & \vdots & \ddots & \vdots \\ J_0(\beta d_{r\,N,1}) & J_0(\beta d_{r\,N,2}) & \cdots & J_0(\beta d_{r\,N,N}) \end{bmatrix} \tag{10}$$

$$\rho_{tx\,n,a} = \begin{bmatrix} J_0(\beta d_{t\,1,1}) & J_0(\beta d_{t\,1,1}) & \cdots & J_0(\beta d_{t\,1,M}) \\ J_0(\beta d_{t\,2,1}) & J_0(\beta d_{t\,2,1}) & \cdots & J_0(\beta d_{t\,2,M}) \\ \vdots & \vdots & \ddots & \vdots \\ J_0(\beta d_{t\,M,1}) & J_0(\beta d_{t\,M,2}) & \cdots & J_0(\beta d_{t\,M,M}) \end{bmatrix} \tag{11}$$

After determining the spatial correlation, the MIMO channel matrix H that accommodates the spatial correlation can be determined using the Kronecker product relation in Equation 12 [10];

$$E\{vec(H)vec(H)^H\} = \rho_{rx} \otimes \rho_{tx} \tag{12}$$

where ρ_{rx} is the spatial correlation matrix in the receiver antenna and ρ_{tx} is the spatial correlation matrix in the transmitter antenna. Using the eigenvalue and eigenvector of $\rho_{rx} \otimes \rho_{tx}$ the $vec(H)$ can be calculated as Equation 13:

$$vec(H) = VD^{1/2} vec(r) \tag{13}$$

where V is a matrix column from the eigenvector of $\rho_{rx} \otimes \rho_{tx}$, D is the diagonal matrix in which the diagonal elements are the eigenvalues of $\rho_{rx} \otimes \rho_{tx}$ and r is a vector containing independent and identically distributed (i.i.d.) complex Gaussian random numbers with a zero mean and a unit variance. $Vec(H)$ has a length of N x M and consists of each column of the correlation matrix H can be constructed as Equation 14:

$$H_{sc} = \begin{bmatrix} vec(H)_1 & vec(H)_{N+1} & \cdots & vec(H)_{N(M-1)+1} \\ vec(H)_2 & vec(H)_{N+2} & & vec(H)_{N(M-1)+2} \\ \vdots & & \ddots & \vdots \\ vec(H)_N & vec(H)_{2N} & \cdots & vec(H)_{NM} \end{bmatrix} \tag{14}$$

The electromagnetic interaction between antennas in an array is expressed as mutual coupling. The mutual coupling between antennas in an array affects the MIMO system's performance. The influence of mutual coupling on MIMO capacity has been examined in many previous studies [14-18]. The modelling of the channel matrix for MIMO, which accounts for mutual coupling, is addressed in references [14, 18]. Regarding the signal power factor in evaluating MIMO capacity, mutual coupling across antennas has been observed to influence the antenna impedance. This then influences the matching condition at the antenna port and may diminish radiation efficiency [19]. Previous studies indicated that mutual coupling among MIMO antennas' antennae affects channel correlation. The correlation with the elaborated mutual coupling effect is diminished compared to when the mutual coupling effect is disregarded [13]. Mutual coupling between antennas in MIMO reduces MIMO channel capacity [14]. The antenna's radiation characteristics affected the mutual coupling, including pattern, polarization, and scattering aperture. Previous research has also addressed the polarization aspect in MIMO antennas to enhance variety [31-35]. The polarization influence on MIMO capacity is analyzed about antenna mutual coupling. The mutual coupling between the antennas on the transmitter side differs from that on the receiver side. The input signal is connected to an adjacent antenna on the transmitter side. When the mutual coupling between antenna elements in both the transmitting and receiving antennas is defined as C_t and C_r. The correlation matrices for the transmitting and receiving antennas can be adjusted as Equations 15 and 16:

$$\rho_{tx\_mc} = \rho_{tx}^{1/2} C_t \tag{15}$$

$$\rho_{rx\_mc} = C_r \rho_{rx}^{1/2} \tag{16}$$

The mutual impedance is usually used to express the mutual coupling effect. Therefore, the C_t and C_r can be determined based on mutual impedance between antenna elements, as written in Equation 17, with Z being matrix impedance, as written in Equation 18 [18]. Z_{ab} is the mutual impedance between a^{th} element and b^{th} elements, Z_s is source impedance, and Z_{in} is an antenna self-impedance, $C_t = (Z_{in} + Z_L)$, and I_M is the identity matrix of size MIMO.

$$C_t = (Z_{in} + Z_L)(Z + Z_L I_M)^{-1} \tag{17}$$

$$Z = \begin{bmatrix} Z_{in} + Z_L & Z_{ab} & \cdots & Z_{aM} \\ Z_{ba} & Z_{in} + Z_L & \cdots & Z_{bM} \\ \vdots & \vdots & \ddots & \vdots \\ Z_{Ma} & Z_{Mb} & \cdots & Z_{in} + Z_L \end{bmatrix} \tag{18}$$

As discussed by Li et al. [17] and Ullah et al. [34], the MIMO channel capacity can be determined in terms of spectral efficiency by using Equation 19 with H_{mc} is MIMO channel matrix described in (H_{mc}) which, considering the mutual coupling, I_N is the identity matrix with the size of MIMO size rank and SNR is the signal-to-noise ratio condition,

$$\boldsymbol{C = E\left\{log_2 \mathrm{det}\left(I_N + \frac{SNR}{M} H_{mc} H_{mc}^H\right)\right\}} \tag{19}$$

This study employs linear polarization. Circular polarization develops from the superposition of phase-differentiated linear polarization. Consequently, linear polarization can also represent circular polarization. This approach simplifies the derivation of the mutual coupling value concerning the polarization difference angle or mismatch. The theta angle, representing the polarization mismatch, eventually influences mutual coupling and channel capacity. The alignment of electromagnetic wave polarization with antenna polarization enhances the received power. Consequently, the mutual coupling between antennas is likewise affected by polarization. Maximum mutual coupling occurs when two antennas have identical co-polarized polarization orientations. Minimum mutual coupling occurs when the polarization of two antennas is orthogonal, specifically cross-polarized. This study employs a MIMO configuration of two Dipole antennas to examine the impact of antenna polarization on MIMO capacity.

Figure 2 illustrates the MIMO antenna. Antenna polarization is associated with antenna orientation. Consequently, the polarization configuration can be established by ascertaining the antenna orientation. Additionally, the mutual impedance between two Dipole antennas with arbitrary orientations can be computed using Equation 20, where Z'_{mn} represents the mutual impedance between the m and n^{th} Dipole elements at a specific distance, as obtained in Gustafsson et al. [18]. Parameters θ_1 and θ_2 represent the orientation of each antenna relative to the position vector connecting the center points of the two antennas. The parameter d_λ denotes the distance between antennas in terms of λ [19]. The mutual impedance in Equation 20 indicates that the polarization configuration will influence the mutual coupling between antennas. The antenna direction indicated by θ signifies the antenna polarization. The mutual impedance between the antennas depicted in Figure 2 will reach its maximum when the two antennas are oriented in parallel. The smallest value will be achieved when the antennas are orthogonal. The parallel alignment of antenna elements can be regarded as a co-polarized state. The perpendicular alignment of antenna elements can be considered as a cross-polarized state. Considering Equation 12, the MIMO channel matrix H_{mc} is influenced by the mutual impedance between MIMO antennas, denoted as C_t and C_r, which is determined by the impedance matrix of the transmitting and receiving antennas. Under cross-polarized conditions, the mutual impedance attains the minimum and maximum values observed in co-polarized conditions. Consequently, the theoretical analysis presented in this section concludes that the polarization configuration affects the MIMO capacity. The cross-polarized state will result in the mutual impedance between elements approaching zero. When the impedances of the transmitting and receiving antennas are matched, the coupling matrix (C_t and C_r) approaches the identity matrix, and the channel matrix is solely affected by spatial correlation. Furthermore, numerical simulations examine the impact of polarization on MIMO capacity. Section 3 addresses the numerical simulation. The research findings about the polarization effect on MIMO capacity can inform decisions regarding antenna orientation or placement in the design of a MIMO antenna system.

$$Z_{mn} = Z'_{mn} \sin(\theta_1)\sin(\theta_2) e^{-j\beta d_\lambda} \tag{20}$$

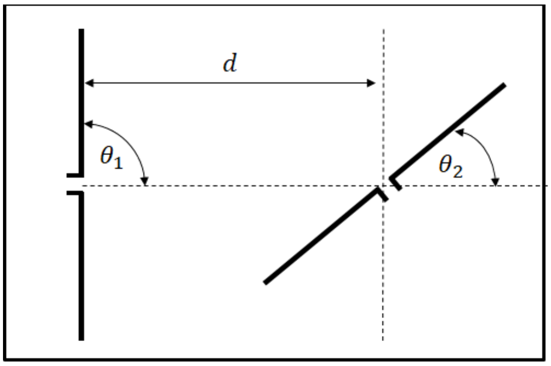

Figure 2. Two Dipole antennas with different orientations (Antennas for All Applications, John D. Krauss)

3- Results and Discussion

Numerical simulations have been carried out following the theoretical analyses described in Section 2. The antenna array comprises multiple half-wavelength Dipole antennas for transmitting and receiving in a MIMO system. The antenna's polarization is established by modifying the relative angles between the elements. A MIMO antenna has two Dipole antenna elements spaced by a distance d, as seen in Figure 2. The orientations of Antenna-1 and Antenna-2 are denoted by θ_1 and θ_2, respectively. It is important to recognize that θ_1 and θ_2 denote the polarization states of Antenna-1 and Antenna-2, respectively. The values of θ_1 and θ_2 may range from 0° to 90°. The distance (d) between antennas is half the wavelength, and the minimal separation between antennas for collinear alignment. This research employs multiple simulation scenarios, with the MIMO antenna configurations presented in Figure 3.

Then, numerical simulations are conducted based on the computation of the estimated channel capacity, Equation 19, addressed in Section 2. Numerical simulations are then performed to ascertain the i.i.d. channel matrix in the evaluated MIMO system. The subsequent step involves generating the correlation matrix as defined in Equations 10 and 11, followed by the computation of mutual impedance using Equation 20. The obtained mutual impedance value is utilized to formulate the impedance matrix at both the transmitting and receiving antennas, consequently facilitating the determination of the mutual coupling matrix. After acquiring the mutual coupling matrix, the next phase involves ascertaining the channel matrix by consulting Equations 12 to 14. This study employs a numerical simulation technique for MIMO systems under i.i.d. channel conditions, incorporating spatial correlation as outlined in Yunita et al. [35]. This numerical simulation program examines the impact of antenna polarization configurations on MIMO channel capacity.

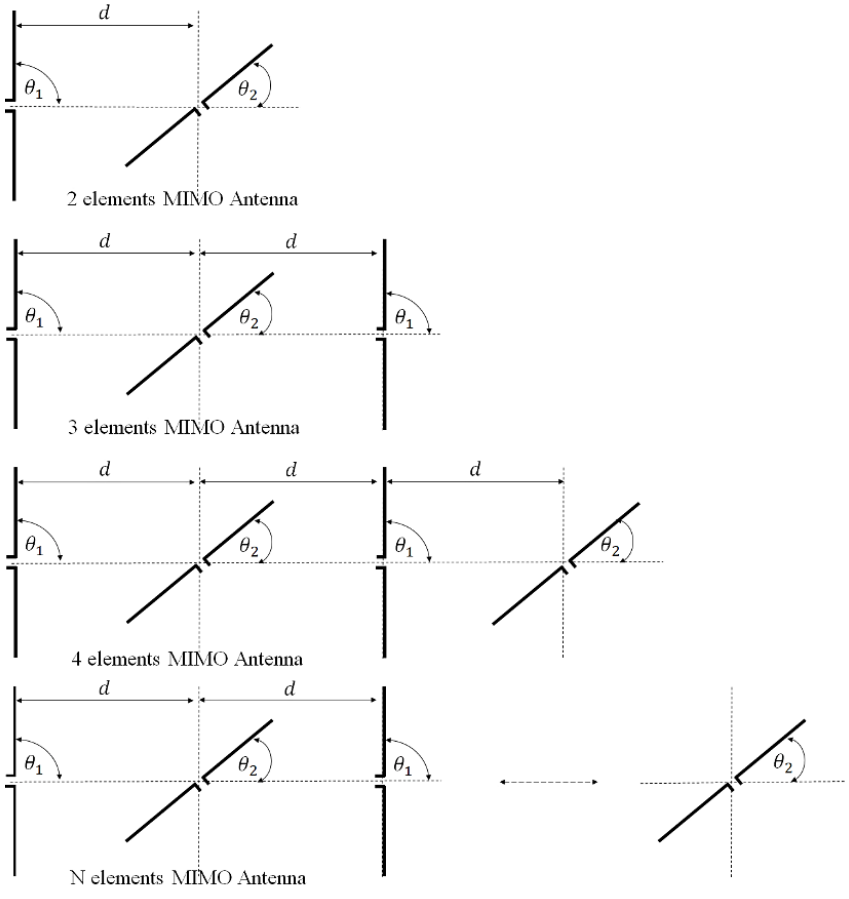

Figure 3. Illustration of the polarization arrangement at several MIMO antennas with different numbers of Dipole antenna elements

The preliminary simulation scenario included a 2×2 MIMO antenna, including two Dipole elements, as seen in Figure 4, utilized at both the transmitter and receiver. This simulation scenario evaluates performance under various SNR conditions, ranging from low to high values. The mutual impedance of the antennas can be calculated using Equation 20. The spatial correlation can be computed using Equations 8 – 10 about the distance d. Consequently, the whole channel matrix illustrating spatial correlations can be obtained by referring to Equation 15. The minimum ergodic capacity of the MIMO system can be determined from Equation 16 by averaging the simulated capacity across the iterations. This study assesses the capability of the MIMO channel in spectral efficiency. This highlights the effect of each element mutual coupling through a comparative study using findings derived exclusively from the i.i.d. channel and spatial correlation, as referenced in Yunita et al. [35]. The results are illustrated in Figure 4. Figure 4 depicts the relationship between spectral efficiency (bps/Hz) and SNR (dB) across three distinct channel types: H_{iid} (solid line), which shows the highest spectral efficiency; H_{sc} (dashed line), indicating moderate efficiency but slightly below the value of H_{iid}, and H_{mc} (long dashed line), reflecting the lowest spectral efficiency. An elevated SNR is associated with enhanced spectral efficiency. H_{iid} demonstrates ideal performance, whereas H_{mc} has the lowest spectral efficiency. The correlation value between antenna elements influences the spectral efficiency, approaching optimum conditions. The anticipated capacity is reduced when considering the effects of mutual coupling among antenna elements in a MIMO antenna, as opposed to a scenario without mutual coupling. The polarization orientation of the two antenna elements affects mutual coupling, hence influencing the achievement of MIMO capacity.

A further investigation was conducted with the second simulated scenario, employing the identical MIMO antenna setup as the initial scenario. This scenario examines the impact of antenna orientation on the MIMO capacity that the antenna can consider. The angle θ_1 was fixed at 90^o, whereas θ_2 was adjusted from 0^o to 90^o. The fluctuation of the θ_2 value denotes the polarization orientation of antenna-2 relative to antenna-1. Figure 5 illustrates the simulation outcomes of the 2×2, 4×4, and 8×8 MIMO systems, with an inter-antenna distance (d) of 0.5 λ, evaluated under an SNR of 25 dB. The results indicate that the optimal channel capacity for each tested MIMO antenna configuration occurs at a θ_2 value of zero. This suggests that the maximum channel capacity is attained in cross-polarization conditions. The minimum capacity is observed under co-polarization conditions. The orientation of the two Dipole antennas depicted in Figure 1 illustrates the polarization characteristics of each antenna. The orientation arrangement corresponds to the polarization arrangement. The relationship between θ_1, θ_2, and mutual impedance, as outlined in Equation 20, indicates that mutual impedance is affected by variations in θ. Modifying antenna polarization affects the mutual impedance between the two antennas, ultimately impacting the MIMO capacity.

The mutual impedance of two Dipole antennas in cross-polarization conditions is lower than that in co-polarization. The change in mutual impedance will influence the channel matrix H_{mc}. The results presented in Figure 5 indicate that the 2×2 MIMO achieves a spectral efficiency of 11.25 bps/Hz for cross-polarization and 10.95 bps/Hz for co-polarization. The enhancement in MIMO capacity achieved through the regulation of antenna polarization is approximately 0.3 bps/Hz. Capacity enhancement is also evident in the results of 4×4 and 8×8 MIMO configurations. The enhancement in capacity was achieved by adjusting the polarization orientation between neighbouring elements in MIMO from co-polarization to cross-polarization. The improvements for 4×4 and 8×8 MIMO are 2.48 bps/Hz and 11.2 bps/Hz, respectively. Capacity reduction can occur if the optimal antenna polarization is not taken into consideration as well. The polarization arrangement is more critical in larger MIMO antenna sizes. The variation in MIMO capacity between optimal and suboptimal orientations is enhanced under high SNR conditions. In low SNR conditions, the difference in MIMO capacity between optimal and suboptimal polarization orientations is minimal for 2×2 MIMO systems.

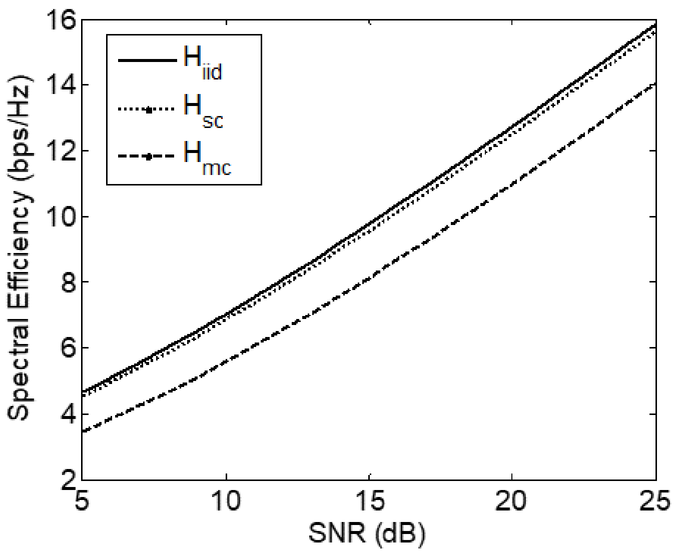

Figure 4. **The simulation results of 2×2 MIMO under three distinct channel scenarios: independent and identically distributed (H_{iid}), spatially correlated (H_{sc}), and with mutual coupling (H_{mc})**

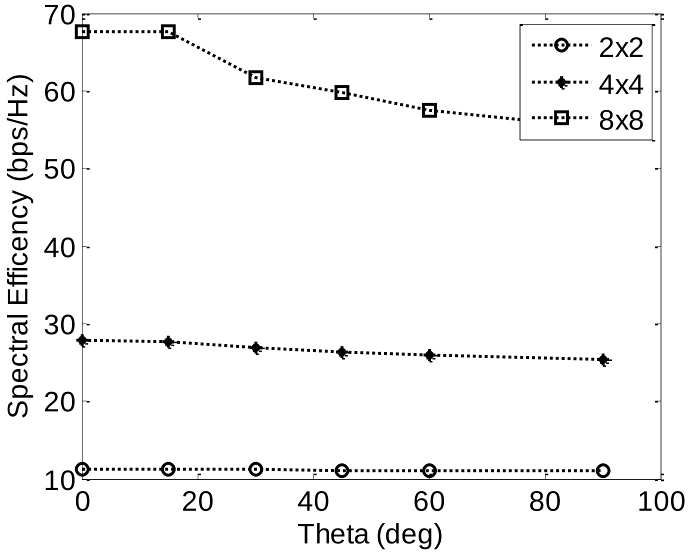

Figure 5. System capacity of MIMO with half-wavelength Dipole elements (d=0.5λ) with varied orientation and numbers of antenna elements

The third simulation scenario assesses the impact of element polarization arrangement on various MIMO antenna systems with different sizes. The simulation begins by exhibiting the polarization configuration on the N-element MIMO antenna in Figure 3. The impact of a polarization arrangement on the MIMO capacity of a 2×2 MIMO system is seen in Figure 6. The polarization setting's effect yields the most significant gain in channel capacity at a theta angle of 90^o, corresponding to the cross-polarization condition. An SNR of 5 dB indicates a low SNR state, whereas an SNR of 25 dB signifies a high SNR condition. The observed gain in spectral efficiency for SNRs of 5 dB and 25 dB is 0.15 bps/Hz and 0.3 bps/Hz, respectively, compared to co-polarized orientation. The results demonstrate that polarization settings do not substantially affect the 2×2 MIMO system.

Figure 7 presents the test results for the 3×3 MIMO system. The polarization setting's effect yields a maximum increase in channel capacity at the theta angle orientation under cross-polarization conditions. The results validate that cross-polarization scenarios among neighbouring elements can enhance channel capacity to its most significant potential. Observations at a low SNR (5 dB) indicated an enhancement in spectral efficiency of 0.8 bps/Hz. In comparison, observations at a high SNR (25 dB) exhibited an improvement in spectral efficiency of 1 bps/Hz relative to co-polarized orientation. The most severe polarization condition could reduce the channel capacity to 5 bps/Hz at low SNR and 7.2 bps/Hz at high SNR, as assessed using H_{mc} level as a reference point. The results demonstrate that the polarization configuration causes similar effects under both SNR conditions.

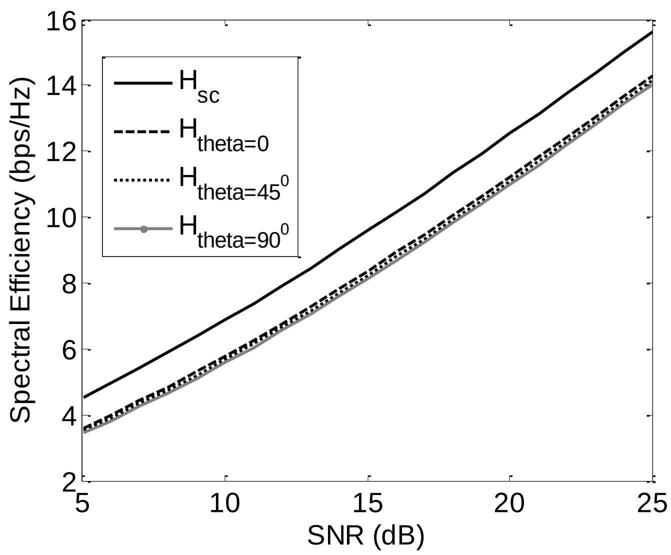

Figure 6. The average capacity of a 2×2 MIMO system using half-wavelength Dipole elements with $d = 0.5\lambda$ and varying SNR levels

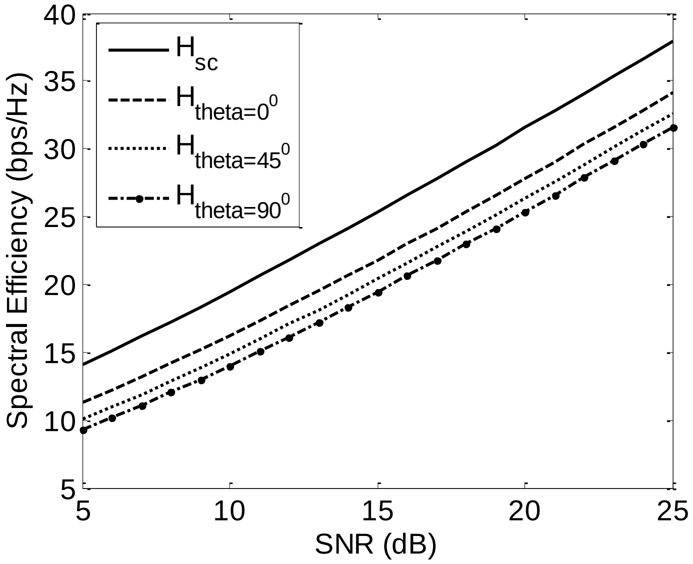

Figure 7. The average capacity of a 3×3 MIMO system using half-wavelength Dipole elements with $d = 0.5\lambda$ and varying SNR levels

Figures 8 and 9 present the results for MIMO systems with configurations of 4×4 and 8×8, respectively. The polarization setting similarly influences the maximum channel capacity increase at the theta angle orientation, specifically under cross-polarization conditions. In a 4×4 MIMO system, observations at low SNR and high SNR indicated an increase in spectral efficiency of 2.12 bps/Hz and 2.45 bps/Hz, respectively. In a 4×4 MIMO system, observations at low and high SNR indicated an increase in spectral efficiency of 9.45 bps/Hz and 11.2 bps/Hz, respectively. The results suggest that the polarization arrangement is more pronounced in both SNR conditions than in MIMO with fewer antennas. The impact of polarization arrangement becomes greater in MIMO systems as the number of antennas increases compared to systems with fewer antennas. The findings in 4×4 and 8×8 MIMO indicate that the most undesirable polarization comes under co-polarized conditions. This condition may lead to a significant degradation in channel capacity when assessed using the H_{mc} level as a baseline. The polarization arrangement must be considered to obtain relevant channel capacity while enhancing MIMO capacity requires an increase in the number of antennas. Increasing the number of antennas in MIMO systems may result in a less substantial increase in capacity if the antennas are not optimally oriented in terms of polarization. This result indicates that the polarization arrangement may effectively reduce capacity loss in MIMO systems. Therefore, it is a critical criterion in designing large MIMO antennas, such as those used in massive MIMO systems. A significant finding is that polarization settings can effectively mitigate noise conditions. Considering the results of the 8×8 MIMO configuration, at a signal-to-noise ratio of 5 dB, the cross-polarized array attains a channel capacity of 32.6 bps/Hz, which is comparable to the channel capacity of the co-polarized array at 11 dB SNR. The results indicate that the cross-polarized array in 8×8 MIMO enhances the SNR by 6 dB. The improvement will be more significant with an increase in the number of antennas, as indicated by the other results. This polarization arrangement method mitigates capacity degradation related to low SNR levels, mainly when more MIMO antenna elements are utilized.

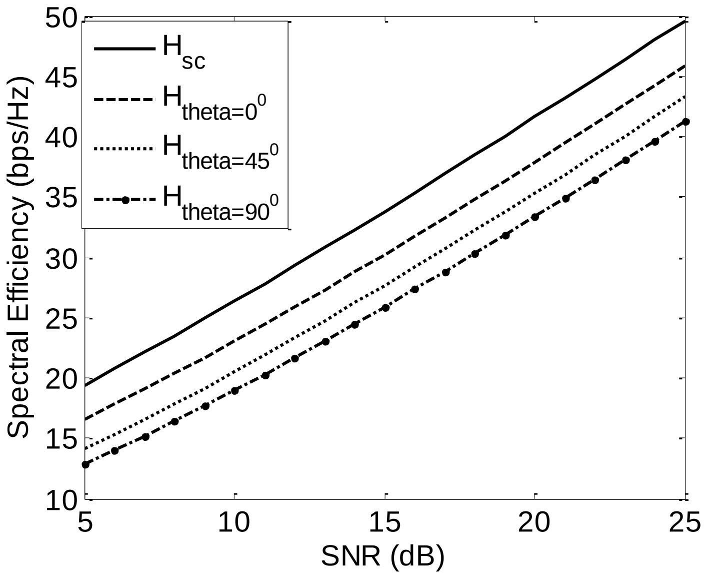

Figure 8. The average capacity of a 4×4 MIMO system using half-wavelength Dipole elements with $d = 0.5\lambda$ and varying SNR levels

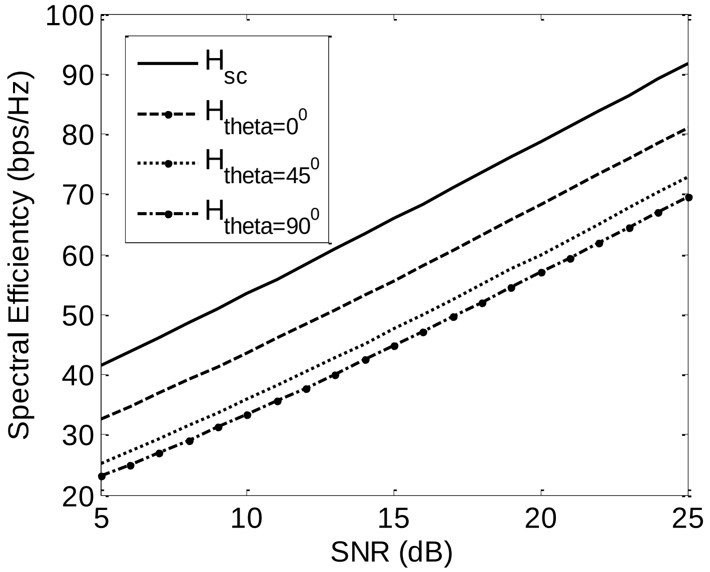

Figure 9. The average capacity of an 8×8 MIMO system using half-wavelength Dipole elements with $d = 0.5\lambda$ and varying SNR levels

4- Conclusion

Theoretical and simulation analyses have been performed regarding the impact of antenna polarization arrangement on the channel capacity of MIMO systems. The results are based on a MIMO antenna model integrating two or more half-wavelength Dipole antennas. The effect of antenna polarization configuration on MIMO capacity is analyzed through variations in antenna orientation. The results indicate that the antenna polarization configuration influences the capacity of the MIMO channel, as demonstrated by both theoretical and simulation studies. Conforming polarization maximizes MIMO channel capacity. Moreover, the results indicate that optimal polarization is achieved in a cross-polarization antenna array with a separation of 0.5λ between antenna elements. The polarization configuration significantly influences MIMO capacity in high SNR conditions. Furthermore, the antenna polarization configuration also significantly influences MIMO capacity in large MIMO systems, regardless of low or high SNR conditions. Simulation results for large MIMO systems indicate that optimal antenna polarization enhances MIMO channel capacity, especially under low SNR conditions. Based on the results, the enhancement of spectral efficiency for MIMO configurations of 2×2, 3×3, 4×4, and 8×8 at low SNR is 0.15 bps/Hz, 0.8 bps/Hz, 2.12 bps/Hz, and 9.45 bps/Hz, respectively. This approach can reduce channel capacity degradation resulting from low SNR levels. However, the enhancement of spectral efficiency for MIMO configurations of 2×2, 3×3, 4×4, and 8×8 at high SNR is 0.3 bps/Hz, 1 bps/Hz, 2.45 bps/Hz, and 11.2 bps/Hz, respectively. The increase in capacity can be attained by modifying the polarization orientation between neighbouring elements in the MIMO antenna. Proper antenna polarization settings are essential in designing large MIMO antennas to align enhanced elements with optimal channel capacity. Then, this study also considers potential trade-offs between optimizing antenna polarization and other design constraints, like physical antenna size or spacing.

5- Declarations

5-1- Author Contributions

Conceptualization, T.Y. and A.A.P.; methodology, T.Y. and A.A.P.; software, A.A.P., T.Y., and H.H.R.; validation, A.A.P., T.Y. and H.H.R.; formal analysis, T.Y. and A.A.P.; investigation, T.Y.; resources, A.A.P.; data curation, A.A.P.; writing—original draft preparation, T.Y.; writing—review and editing, A.A.P. and H.H.R.; visualization, T.Y. and A.A.P.; supervision, A.A.P.; project administration, A.A.P.; funding acquisition, A.A.P. All authors have read and agreed to the published version of the manuscript.

5-2- Data Availability Statement

The data presented in this study are available on request from the corresponding author.

5-3- Funding

This work and publication are partially sponsored by the University Center of Excellence for Intelligent Sensing-IoT, Telkom University, 40257, Indonesia.

5-4- Institutional Review Board Statement

Not applicable.

5-5- Informed Consent Statement

Not applicable.

5-6- Conflicts of Interest

The authors declare that there is no conflict of interest regarding the publication of this manuscript. In addition, the ethical issues, including plagiarism, informed consent, misconduct, data fabrication and/or falsification, double publication and/or submission, and redundancies have been completely observed by the authors.

6- References

[1] Leftah, H. A., & Alminshid, H. N. (2019). Channel capacity and performance evaluation of precoded MIMO-OFDM system with large-size constellation. International Journal of Electrical and Computer Engineering, 9(6), 5024–5030. doi:10.11591/ijece.v9i6.pp5024-5030.

[2] Marzetta, T. L. (2015). Massive MIMO: An introduction. Bell Labs Technical Journal, 20, 11–12. doi:10.15325/BLTJ.2015.2407793.

[3] Rahman, A., Kishore, S., & Rajak, A. A. (2024). Design and Study the Performance of a CMOS-Based Ring Oscillator Architecture for 5G Mobile Communication. Emerging Science Journal, 8(1), 283-296. doi:10.28991/ESJ-2024-08-01-020.

[4] Lu, L., & Sali, A. (2024). Channel Estimation for 29GHz mm Wave MIMO Systems in Tropical Region. 2024 IEEE 7th International Symposium on Telecommunication Technologies: Exploring Future Frontiers in Telecommunication and Vehicular Technologies, ISTT 2024, 48–52. doi:10.1109/ISTT63363.2024.10750580.

[5] Malviya, L., Panigrahi, R. K., & Kartikeyan, M. V. (2020). MIMO Antennas for Wireless Communication. In MIMO Antennas for Wireless Communication. CRC Press, Florida, United States. doi:10.1201/9781003080275.

[6] Ahn, K. S., Heath, R. W., & Baik, H. K. (2008). Shannon capacity and symbol error rate of space-time block codes in MIMO rayleigh channels with channel estimation error. IEEE Transactions on Wireless Communications, 7(1), 324–333. doi:10.1109/TWC.2008.060539.

[7] Subashini, V., Aasitha, S., Brindha, V., Madhumitaa, K., & Rajalakshmi, B. (2024). Design of circular-shaped two-element MIMO antenna for 5G communication. 2024 International Conference on Communication, Computing and Internet of Things, IC3IoT 2024 - Proceedings, 1–5. doi:10.1109/IC3IoT60841.2024.10550339.

[8] Irshad Ali, T. K., Ansal, K. A., Jagadish Chandran, G., Ragesh, G. K., & Mathew, S. (2024). MIMO Antenna Design for Wireless Communication: A Review on Design Challenges and Isolation Techniques. 2024 1st International Conference on Trends in Engineering Systems and Technologies, ICTEST 2024, 1–6. doi:10.1109/ICTEST60614.2024.10576148.

[9] Samimi, M. K., Sun, S., & Rappaport, T. S. (2016). MIMO channel modeling and capacity analysis for 5G millimeter-wave wireless systems. 2016 10th European Conference on Antennas and Propagation, EuCAP 2016, 1–5. doi:10.1109/EuCAP.2016.7481507.

[10] De Flaviis, F., Jofre, L., Romeu, J., & Grau, A. (2008). Multiantenna systems for MIMO communications. In Synthesis Lectures on Antennas. Multiantenna Systems for MIMO Communications. Morgan Claypool Publishers, California, United States. doi:10.2200/S00104ED1V01Y200803ANT007.

[11] Liu, X., & Bialkowski, M. E. (2010). Effect of antenna mutual coupling on MIMO channel estimation and capacity. International Journal of Antennas and Propagation, 306173, 1–4. doi:10.1155/2010/306173.

[12] Mistialustina, H., Yunita, T., Imelda Uli Vistalina, S., Chairunnisa, Pramudita, A. A., & Munir, A. (2023). Performance Evaluation of MIMO Channel Capacity Based on Polarization Loss Factor. Proceedings - 2023 28th Asia Pacific Conference on Communications, APCC 2023, 412–415. doi:10.1109/APCC60132.2023.10460721.

[13] Hui, H. T. (2009). Influence of antenna characteristics on MIMO systems with compact monopole arrays. IEEE Antennas and Wireless Propagation Letters, 8, 133–136. doi:10.1109/LAWP.2009.2012446.

[14] Chen, X., Zhang, S., & Li, Q. (2018). A Review of Mutual Coupling in MIMO Systems. IEEE Access, 6, 24706–24719. doi:10.1109/ACCESS.2018.2830653.

[15] Chen, K. H., & Kiang, J. F. (2016). Effect of mutual coupling on the channel capacity of MIMO systems. IEEE Transactions on Vehicular Technology, 65(1), 398–403. doi:10.1109/TVT.2015.2397033.

[16] Wallace, J. W., & Jensen, M. A. (2004). Mutual coupling in MIMO wireless systems: A rigorous network theory analysis. IEEE Transactions on Wireless Communications, 3(4), 1317–1325. doi:10.1109/TWC.2004.830854.

[17] Li, X., & Nie, Z. P. (2004). Mutual coupling effects on the performance of MIMO wireless channels. IEEE Antennas and Wireless Propagation Letters, 3(1), 344–347. doi:10.1109/LAWP.2004.840252.

[18] Gustafsson, M., Aulin, J., Hogberg, M., Alm, M., & Sihlbom, B. (2014). Impact of mutual coupling on capacity in large MIMO antenna arrays. 8th European Conference on Antennas and Propagation, EuCAP 2014, 2723–2727. doi:10.1109/EuCAP.2014.6902387.

[19] Dkiouak, A., Zakriti, A., Ouahabi, M. El, Touhami, N. A., & Mchbal, A. (2019). Design of a four-element MIMO antenna with low mutual coupling in a small size for satellite applications. Progress in Electromagnetics Research M, 85, 95–104. doi:10.2528/pierm19071202.

[20] Ghimire, J., Choi, K. W., & Choi, D. Y. (2019). Bandwidth enhancement and mutual coupling reduction using a notch and a parasitic structure in a UWB-MIMO Antenna. International Journal of Antennas and Propagation, 8945386, 1–9. doi:10.1155/2019/8945386.

[21] Liu, Y., Yang, X., Jia, Y., & Guo, Y. J. (2019). A Low Correlation and Mutual Coupling MIMO Antenna. IEEE Access, 7, 127384–127392. doi:10.1109/ACCESS.2019.2939270.

[22] Wang, F., Duan, Z., Li, Q., Wei, Y., & Gong, Y. (2017). Compact wideband MIMO antenna for 5G communication. 2017 IEEE Antennas and Propagation Society International Symposium, Proceedings, 2017-January, 939–940. doi:10.1109/APUSNCURSINRSM.2017.8072512.

[23] Zhang, W., Weng, Z., & Wang, L. (2018). Design of a dual-band MIMO antenna for 5G smartphone application. 2018 IEEE International Workshop on Antenna Technology, IWAT2018 - Proceedings, 1–3. doi:10.1109/IWAT.2018.8379211.

[24] Ahmad, S., Shah, S. T., Durani, M. H., & Denidni, T. A. (2024). Octa-Port MIMO Antenna System for 5G Smartphone Applications. IEEE Antennas and Propagation Society, AP-S International Symposium (Digest), 877–878. doi:10.1109/AP-S/INC-USNC-URSI52054.2024.10686757.

[25] Han, G., Han, L., Ma, R., Zeng, Q., & Zhang, W. (2016). A novel MIMO antenna with DGS for high isolation. 2016 IEEE MTT-S International Conference on Numerical Electromagnetic and Multiphysics Modeling and Optimization, NEMO 2016, 1–2. doi:10.1109/NEMO.2016.7561671.

[26] Yin, B., Feng, X., & Gu, J. (2020). A Metasurface Wall for Isolation Enhancement: Minimizing mutual coupling between MIMO antenna elements. IEEE Antennas and Propagation Magazine, 62(1), 14–22. doi:10.1109/MAP.2019.2943299.

[27] Dadgarpour, A., Zarghooni, B., Virdee, B. S., Denidni, T. A., & Kishk, A. A. (2017). Mutual Coupling Reduction in Dielectric Resonator Antennas Using Metasurface Shield for 60-GHz MIMO Systems. IEEE Antennas and Wireless Propagation Letters, 16, 477–480. doi:10.1109/LAWP.2016.2585127.

[28] Ding, C. F., Zhang, X. Y., Xue, C. D., & Sim, C. Y. D. (2018). Novel Pattern-Diversity-Based Decoupling Method and Its Application to Multielement MIMO Antenna. IEEE Transactions on Antennas and Propagation, 66(10), 4976–4985. doi:10.1109/TAP.2018.2851380.

[29] Zhang, Y. M., Zhang, S., Li, J. L., & Pedersen, G. F. (2019). A Transmission-Line-Based Decoupling Method for MIMO Antenna Arrays. IEEE Transactions on Antennas and Propagation, 67(5), 3117–3131. doi:10.1109/TAP.2019.2900406.

[30] Pramudita, A. A., Yunita, T., Alia, D., & Sholihin. (2020). MIMO antenna for IEEE 802.11ac with cross-polarized circular configuration of printed Yagi elements. International Journal on Communications Antenna and Propagation, 10(4), 240–248. doi:10.15866/irecap.v10i4.18223.

[31] Sharma, Y., Sarkar, D., Saurav, K., & Srivastava, K. V. (2017). Three-Element MIMO Antenna System with Pattern and Polarization Diversity for WLAN Applications. IEEE Antennas and Wireless Propagation Letters, 16, 1163–1166. doi:10.1109/LAWP.2016.2626394.

[32] Chakraborty, S., Rahman, M. A., Hossain, M. A., Mobashsher, A. T., Nishiyama, E., & Toyoda, I. (2019). Design and performance studies of a MIMO antenna with circular polarization diversity for 5G applications. 2019 5th International Conference on Advances in Electrical Engineering, ICAEE 2019, 128–133. doi:10.1109/ICAEE48663.2019.8975509.

[33] Umaisaroh, U., Hendrantoro, G., Mauludiyanto, A., & Fukusako, T. (2019). Capacity of 2 2 MIMO HF NVIS Channels with Linearly Polarized Horizontal Antennas. IEEE Wireless Communications Letters, 8(4), 1120–1123. doi:10.1109/LWC.2019.2908648.

[34] Ullah, U., Mabrouk, I. Ben, & Koziel, S. (2020). Enhanced-performance circularly polarized MIMO antenna with polarization/pattern diversity. IEEE Access, 8, 11887–11895. doi:10.1109/ACCESS.2020.2966052.

[35] Yunita, T., Chairunnisa, Pramudita, A. A., & Munir, A. (2024). Effect of Polarization Loss on Channel Capacity. Lecture Notes on Data Engineering and Communications Technologies, 186, 282–291. doi:10.1007/978-3-031-46784-4_27.